Enhanced emission of intermediate/semi-volatile organic matters in both gas and particle phases from ship exhausts with low-sulfur fuels

Binyu Xiao[1], Fan Zhang[1,2,*], Zeyu Liu[3], Yan Zhang[4,5], Rui Li[1,2], Can Wu[1,2], Xinyi Wan[1], Yi Wang[1], Yubao Chen[1], Yong Han[6], Min Cui[7], Libo Zhang[8], Yingjun Chen[4,5], Gehui Wang [1,2,*]

[1] Key Lab of Geographic Information Science of the Ministry of Education, School of Geographic Sciences, East China Normal University, Shanghai, 200241, China

[2] Institute of Eco-Chongming, 20 Cuiniao Road, Chongming, Shanghai, 202150, China

[3] State Key Laboratory of Loess and Quaternary Geology, Institute of Earth Environment, Chinese Academy of Sciences, Xi'an 710061, China

[4] Shanghai Key Laboratory of Atmospheric Particle Pollution and Prevention (LAP3), Department of Environmental Science and Engineering, Fudan University, Shanghai, 200438, China

[5]Shanghai Institute of Pollution Control and Ecological Security, Shanghai, 200092, China

[6] Department of Civil and Environmental Engineering and State Key Laboratory of Marine Pollution, The Hong Kong Polytechnic University, Kowloon, Hong Kong

[7] College of Environmental Science and Engineering, Yangzhou University, Yangzhou, 225009, China

[8] No.1 Drilling Company, Great Wall Drilling Company, China National Petroleum Corporation, Panjin, 124010, China

Corresponding Authors: Fan Zhang (fzhang@geo.ecnu.edu.cn) and Gehui Wang (ghwang@geo.ecnu.edu.cn)

Abstract

The widespread utilization of low-sulfur fuels in compliance with global sulfur limit regulations has significantly mitigated the emissions of sulfur dioxide (SO_2) and particulate matter (PM) on ships. However, significant uncertainties still persist

regarding the impact on intermediate/semi-volatile organic compounds (I/SVOCs). Therefore, on-board test of I/SVOCs from three ocean-going vessels (OGVs) and four inland cargo ships (ICSs) with low-sulfur fuels (< 0.50% m/m) in China were carried out in this study. Results showed that the emission factors of total I/SVOCs were 881 ± 487, 1181 ± 421 and 1834 ± 667 mg (kg fuel)$^{-1}$ for OGVs with heavy fuel oil (HFO), marine gas oil (MGO) and ICSs with 0# diesel, respectively. The transition from low-sulfur content (< 0.50% m/m) to ultra-low-sulfur content (< 0.10% m/m) fuels had evidently enhanced the emission factor of I/SVOCs, with non-ignorable contribution from particle-phase I/SVOCs, thereby further amplifying the secondary organic aerosol formation potential (SOAFP). Fuel type, engine type, and operating conditions comprehensively influenced the emission factor level, compositions, and volatility distribution of I/SVOCs. Notably, a substantial proportion of fatty acids had been identified in ship exhausts, necessitating heightened attention. Furthermore, organic diagnostic markers of hopanes, in conjunction with the $C_{18:0}$ to $C_{14:0}$ acid ratio, could be considered as potential markers for HFO exhausts. The findings suggest that there is a necessity to optimize the implementation of a global policy on ultra-low-sulfur oil in the near future.

Keywords: ship emission, I/SVOCs, low-sulfur fuel, SOAFP

1 Introduction

Ship transportation plays a critical role in global trade, as it accounts for over 80% of the total cargo transport worldwide due to its substantial carrying capacity and cost-effectiveness (Zhang et al., 2016;Zhang et al., 2021). Consequently, the expansion of the global economy has led to an increasing impact on air quality, human health, and various other aspects due to the emission of gaseous and particulate pollutants from ship exhausts (Zhang et al., 2018a;Zhang et al., 2014;Liu et al., 2022). Over the past two decades, extensive studies have been carried out on the characteristics of various vessel pollutants, including sulfur dioxide (SO_2), nitrogen oxide (NO_x), particulate matter (PM), carbon dioxide (CO_2) and volatile organic compounds (VOCs) (Davis et al., 2001;Liu et al., 2022). Results show that shipping emissions are responsible for 2%-

5% of fine particulate matter ($PM_{2.5}$) (Kramel et al., 2021); CO_2 from ships accounts for around 3% of the total global CO_2 emission (Faber et al., 2020); while the NO_x from ships contributes approximately 15% of the total global atmospheric NO_x emission (Faber et al., 2020). Besides, the employment of high-sulfur fuel (HSF, ≥ 0.50% m/m) has resulted in a significant emission of SO_2 from ship exhausts, which accounts for approximately 14% of global anthropogenic SO_2 emissions (Zhou et al., 2019). Specifically, the consumption of heavy fuel oil constitutes 70% of total ship fuel usage (International Maritime Organization, 2016), which is primarily responsible for the majority of SO_2 emissions associated with global shipping. This has considerable effects on coastal regions and the marine environment. ~~Particularly, the 70% consumpbustion of heavy fuel oil in ships account for the majority of global shipping-related SO_2 emissions,total ship fuel usage accounts for the majority of global shipping-related SO_2 emissions, leading to significant impacts on coastal areas and the marine environment (International Maritime Organization, 2016).~~

Given all this, the International Maritime Organization (IMO, additional abbreviations and their corresponding full names are provided in Supplementary Table S1) has been continuously revising the International Convention for the Prevention of Pollution from Ships (MARPOL) since 1997, progressively imposing stricter sulfur limits on marine fuels. Following the guidelines of Annex VI to the MARPOL, the limit for sulfur content in ship fuels has been set at 0.50% (m/m) since 2020 globally, or alternative measures such as exhaust scrubbers must be employed (International Maritime Organization, 2016). In designated Sulfur Emission Control Areas (SECAs, including the North Sea, the Baltic Sea, North America and the United States Caribbean), this limit has been further restricted to below 0.10% (m/m) since 2015. In certain SECAs, the utilization of exhaust scrubbers as an alternative treatment method to low-sulfur fuel is not even acceptable. Numerous countries are undergoing a transition in their shipping practices, shifting from high-sulfur fuels to low-sulfur or ultra-low sulfur alternatives (Liu et al., 2019;Zhang et al., 2024;Zhang et al., 2021).

Within China, emission standards vary across regions, with specific requirements tailored to each area. Typically, the fuel oil regulations of China may mandate vessels to maintain sulfur content at below either 0.50% (m/m) in SECAs since 2019 or 0.10% (m/m) in inland areas and specific control regions since 2020 when utilizing fuel. In brief, the global mandatory use of ultra-low sulfur content fuel (< 0.1% m/m) or alternative measures is an inevitable trend in the near future.

Previous studies have indicated that the low-sulfur fuel regulation is an effective measure for reducing SO_2 and PM mass emission in many countries. For example, Lehtoranta et al. (2019) demonstrate that the change of fuel from high-sulfur to lower-sulfur has significantly decreased the PM emissions. The global shipping emissions have been quantified by Sofiev et al. (2018) using the Ship Traffic Emissions Assessment Model (STEAM). Their finding reveals a positive correlation between the implementation of sulfur reduced fuel strategy and reductions in both SO_2 and PM levels. However, even though studies have shown that the low-sulfur fuel policy may reduce emissions of PM and SO_2, it could lead to increase of VOCs and intermediate volatile organic compounds (IVOCs) (Sofiev et al., 2018;He et al., 2022a;Shen et al., 2023;Liu et al., 2022). The impact of fuel quality on organic compounds, such as VOCs and intermediate/semi-volatile organic compounds (I/SVOCs), remains significant uncertainty.

VOCs have been getting lots of interests due to their crucial role as common precursors of secondary organic aerosols (SOAs) and ozone (O_3) (Shen et al., 2023;Hui et al., 2019). Additionally, the aging process of VOCs and the resulting intermediates also play pivotal role in SOA formation (He et al., 2023; Srivastava et al., 2022). Recently, numerous studies have unveiled a substantial gap between measured SOAs and theoretical calculated SOAs, with the primary cause being attributed to the neglect of I/SVOCs (Fang et al., 2021;Knote et al., 2015). For example, the study conducted by An et al. (2023) integrates an emission inventory of I/SVOCs into the Community Multiscale Air Quality (CMAQ) modeling system to simulate the characteristics of

primary organic aerosols (POA) and SOAs originating from various sources within the Yangtze River Delta (YRD) region. Their findings reveal a significant 148% increase in predicted SOA concentrations. Wu et al. (2019) employ Weather Research and Forecasting model coupled with Chemistry (WRF-Chem) to organize the 2010 I/SVOCs emission inventory in Pearl River Delta (PRD) region of China, revealing a substantial 161% increase in SOA concentration. However, there is still a significant dearth of measured I/SVOCs from various sources, leading to substantial uncertainty in the estimation of inventory and estimation of SOAs. Clarifying the contribution of I/SVOCs from different sources to SOA formation is crucial for a comprehensive understanding of their role in atmospheric processes and their impact on air quality (He et al., 2024; Srivastava et al., 2022).

In recent years, several studies have reported measured data of organic compounds with varying volatility emitted from ships. Although progress has been achieved in shipping I/SVOCs measurement, a comprehensive understanding of their characteristics and their contribution to SOA formation remains insufficient, particularly in light of increasingly stringent global emission control regulations. Previous studies mainly focus on gas-phase VOCs and IVOCs, which might underestimate the emissions of particle-phase I/SVOCs (Huang et al., 2018a;Zhang et al., 2018b;Zhang et al., 2024). Particulate I/SVOCs can also form SOA after being transferred to the gaseous state through evaporation and undergoing atmospheric oxidation (Srivastava et al., 2022;Liu et al., 2022). And the qualitative analysis of particle-phase I/SVOCs in ship exhaust focuses more on detecting and evaluating of n-alkanes and 16 polycyclic aromatic hydrocarbons (PAHs) based on limited previous studies, with little emphasis on other species of I/SVOCs (Liang et al., 2022;Perrone et al., 2014). In ~~There~~ brief, there is a lack of simultaneous measurement data on detailed low-volatility organic compounds in both gas and particle phases, which could be beneficial to the accurate evaluation of SOA and O_3 formation potentials. Moreover, the effects resulting from the implementation of low-sulfur fuel policies on shipping

I/SVOC emission characteristics remain unclear, particularly regarding the utilization of ultra-low sulfur fuels (≤0.1%, m/m). There is an urgent need to update emission factors and component profiles of full-volatility particulate organic compounds, as this is crucial for reducing uncertainties in I/SVOCs inventory estimation and providing fundamental data for formulating optimal emission control policies for ships, considering their comprehensive impacts on various pollutants.

Therefore, typical ocean-going vessels (OGVs) and inland cargo ships (ICSs) with different types of fuels in China were selected for on-board measurement in this study. Gas-phase and particle-phase I/SVOCs were collected synchronously from ship exhausts with different low-sulfur fuels under different engine conditions. A comprehensive analysis was conducted on the emission factor, volatility, profile, and influence factors of I/SVOCs. Besides, the SOA formation potential (SOAFP) of I/SVOCs from the test ships were also estimated based on the measured data.

2 Material and methods

2.1 Test Ships and Fuels

On-board test of seven typical Chinese cargo ships have been carried out in this study, including three large ocean-going vessels and four small inland cargo ships. Detailed comprehensive parameters of the test ships can be found in Table S2. The OGVs were equipped with two types of engines, one was two-stroke main engine (ME) and the other was four-stroke auxiliary engine (AE). Meanwhile, the ICSs only had one four-stroke main engine. Low-sulfur content heavy fuel oil (HFO) and ultra-low-sulfur marine gas oil (MGO) were used as fuels of OGVs, while 0# diesel with ultra-low-sulfur content was used for ICS engines. The detailed parameters of fuels used in this study are shown in Table 1. It should be acknowledged that all those fuels complied with the latest regulations issued by both IMO and China. The engines tested in this study were not equipped with any aftertreatment devices.

Table 1 Parameters of the fuels used in the test ships.

	Unit	OGV1 /HFO	OGV1 /MGO	OGV2 /HFO	OGV2 /MGO	OGV3 /HFO	OGV3 /MGO	ICS /0# diesel

Gross calorific value	MJ kg^{-1}	44.21	45.76	42.62	45.72	43.08	45.64	
Net calorific value	MJ kg^{-1}	41.45	42.75	40.28	42.71	40.61	42.66	
Kinematic viscosity	(50°C), mm^2/s	44.04						
Kinematic viscosity	(20°C), mm^2/s		5.216	152.3	4.724	161.1	5.363	
Moisture	%m	0.03	N.D.	0.09	N.D.	0.12	N.D.	
Ash	%m							
Sulfur (S)	%m	0.50	0.03	0.43	0.02	0.43	0.05	N.D.
Carbon (C)	%m	86.62	80.80	82.4	79.6	69.9	66.5	85.5
Hydrogen (H)	%m	11.33	8.15	9.68	12.3	11.3	10.61	
Nitrogen (N)	%m	N.D.	N.D.	0.39	N.D.	2.36	N.D.	
Oxygen (O)	%m	0.36	N.D.	1.53	0.59	1.34	0.73	
Vanadium (V)	mg kg^{-1}			N.D.	0.20	4.00	N.D.	
Nickel (Ni)	mg kg^{-1}			16.0	0.10	15.0	N.D.	
Sodium (Na)	mg kg^{-1}			6.00	0.10	8.00	0.10	
Lead (Pb)	mg kg^{-1}			N.D.	0.30	N.D.	N.D.	
Zinc (Zn)	mg kg^{-1}			2.00	0.40	8.00	0.20	
Aluminum + Silicon (Al + Si)	mg kg^{-1}			8.00	0.80	12.0	0.90	

2.2 Sampling system

Real-world measurement of pollutants from vessels under different operating conditions were conducted by a combined sampling system in this study. Vessel exhaust in sampling was passed through a dilution system followed by various connected samplers (Figure S1). Detailed information was described in previous studies (Zhang et al., 2016;Zhang et al., 2024). Briefly, two separate sampling pipes were utilized to direct emissions from the main engine and auxiliary engine stacks, respectively. A flue gas analyzer probe (Testo 350, testo, Germany) was then inserted into the sampling pipe to directly measure gaseous pollutants for online data collection (CO_2, O_2, CO, NO, NO_2, SO_2). Another probe was used to extract flue gas for dilution. PM samples (total suspended particles) were collected using particulate samplers, while gas samples were obtained by employing polyurethane foam. In this study, the dilution ratios varied from 1 to 10 according to operating conditions. A total of 64 sets of gas-phase and particle-phase I/SVOCs samples were collected in this study, involving various engine types, fuels, and operating modes (Table S3). Offline samples were wrapped in prebaked

aluminum foil and stored at -20°C until analysis. Additionally, all samples were analyzed within two weeks of sampling.

2.3 Chemical analysis

Organic matters in both gas-phase and particle-phase samples in this study were analyzed by a gas chromatography - mass spectrometry (GC-MS, Agilent GC 7890B/MS 5977B, HP-5MS). Prior to analysis, the organic fraction was subjected to the analytical method of N, O-bis (trimethylsilyl) trifluoroacetamide (BSTFA) derivatization and spiked with internal standard (tridecane, 3.024 ng/uL). The qualitative analysis was conducted using the National Institute of Standards and Technology (NIST) standard organic mass spectral library queries, in conjunction with their standard compound retention time. Detailed information of analysis and detection process has been described elsewhere (Li et al., 2020;Li et al., 2016).

A total of 76 specific I/SVOC species were identified and quantified in this study, including 24 n-alkanes (C_{12}-C_{36}), 16 polycyclic aromatic hydrocarbons (PAHs), 8 oxygenated polycyclic aromatic hydrocarbons (OPAHs), 17 acids (13 fatty acids and 3 benzoic acids) and 11 hopanes. Detailed information about the identified I/SVOC species were presented in Table S4. Furthermore, the quantification of branched alkanes (b-alkanes) and unresolved complex mixtures (UCMs) were conducted using a procedure described by previous studies (Zhao et al., 2016;Zhao et al., 2014). Given the good linear relationship between carbon number and volatility of n-alkanes, relative response factor (RRF) of n-alkanes were used as the surrogate for b-alkanes and UCMs to estimate their concentrations. The volatility classification of each substance is distinguished based on its carbon number. Generally, compounds with carbon numbers of 12–22 (C_{12}-C_{22}) are classified as IVOCs, while those with carbon numbers of 23–36 (C_{23}-C_{36}) are considered SVOCs (Zhao et al., 2014;Fujitani et al., 2020).

2.4 Emission Factor

Fuel-based emission factors were provided and discussed in this study using the carbon balance method. It is assumed that, under ideal conditions, all carbon in the fuel will undergo complete conversion into carbon present in CO_2, CO, organic carbon (OC),

and elemental carbon (EC) following combustion. OC and EC were analyzed using an OC/EC analyzer (Model 4, Sunshine Lab). The CO_2 emission factor was derived using the following formula.:

$$EF_{CO_2} = \frac{c_F \times \Delta(CO_2)}{\Delta(c_{CO_2}) + \Delta(c_{CO}) + \Delta(c_{OC}) + \Delta(c_{EC})} \quad (1)$$

where EF_{CO_2} is the emission factor of CO_2 (g (kg fuel)$^{-1}$); $\Delta(CO_2)$ indicates the CO_2 mass level after adjustment for environmental background (g m^{-3}); and c_F is the carbon content of fuel (g (kg fuel)$^{-1}$) ; $\Delta(c_{CO_2})$, $\Delta(c_{CO})$, $\Delta(c_{OC})$ and $\Delta(c_{EC})$ represent the mass carbon concentrations of CO_2, CO, OC and EC following the deduction of the background (g m^{-3}), respectively.

$$EF_x = \frac{\Delta X_x}{\Delta CO_2} \times \frac{M_x}{M_{CO_2}} \times EF_{CO_2} \quad (2)$$

where EF_x (g (kg fuel)$^{-1}$) represents the emission factor for species x; ΔX_x and ΔCO_2 (mol m^{-3}) are the concentrations of species x and CO_2 after background correcting; and M_x and M_{CO_2} express the molecular weights of species x and CO_2, respectively.

2.5 SOA formation potential

The organic compounds in this study were categorized into two classes based on volatility: Bin12-22 were defined as IVOCs, and Bin23-36 were defined as SVOCs, corresponding to C12-22 and C23-36, respectively. The equation utilized for the estimation of SOA production via IVOCs in this study is as follows:

$$\Delta SOA_{IVOCs} = \sum_j [HC_j] \left(1 - e^{-k_{OH,j}[OH]\Delta t}\right) \times Y_j \quad (3)$$

where $[HC_j]$ represents the concentration of IVOCs species involved in the reaction, Y_j is the yield coefficient of IVOCs species, and k_{OH}- is the OH reaction rate constant of precursor j at 25°C (cm^3·molecules^{-1}·s^{-1}); [OH] is the OH concentration (molecules·cm^{-3}), which is assumed in this study to be 1.5×10^6 molecules·cm^{-3}; Δt is the photochemical age (h); and Y_j is the SOA mass yield of precursor *j*. And the OH reaction rate constants (cm^3 molec^{-1} s^{-1}) and SOA yields used in this study were the same as Zhao et al. (2016), which reacted (Δt) after 48 h photo-oxidation at the OA

concentration of 9 μg/m^3, the specific values of Y_j and k_{OH} under different environmental conditions were obtained from the simulation study of smoke chamber (Table S5-S6).

The equation for estimating SOA yield based on SVOCs is as follows:

$$\Delta SOA_{SVOCs} = \sum_j (\Delta X_j \cdot Y_j) \quad (4)$$

where ΔX_j is the reaction mass of the compound in the j interval after partitioning, based on its saturation concentration, and Y_j is the respective SOA yield. The study employed a conservative calculation method and identified the UCM as the n-alkane component with the lowest SOA yield. Additionally, the yield coefficients of C23 and higher, which were not included in the relevant parameters, were cautiously replaced with those of C22.

2.6 Quality Assurance and Quality Control

PAHs stipulated by EPA in the United States were used for recovery experiments, and the recovery rate of PAHs was 82% ~ 115%. Before conducting GC-MS measurements, n-hexane was injected prior to each measurement in order to ensure a stable baseline and clean column. Subsequently, standard samples were introduced into the instrument for calibration purposes. The quantitative error of the target compound concentration was ensured to be less than 5% by randomly re-testing one sample after every 20 samples. Moreover, the calibration of target compounds was performed through simultaneous measurement of blank samples to eliminate any potential experimental contamination.

3 Results and discussion

3.1 Emission factors for total I/SVOCs ($EF_{I/SVOCs}$)

Figure 1 presents the total $EF_{I/SVOCs}$ in both gas and particle phases for OGVs and ICSs under different engine types and fuels. Obviously, OGVs had lower I/SVOCs emission factors than ICSs. The average total EF_{IVOCs} of OGVs and ICSs were 512 ± 292 mg (kg fuel)$^{-1}$ and 784 ± 517 mg (kg fuel)$^{-1}$, respectively. While the average total EF_{SVOCs} of OGVs and ICSs were 520 ± 268 mg (kg fuel)$^{-1}$ and 1050 ± 817 mg (kg fuel)$^{-}$

269 ^{1}, respectively. The ICSs with 0# diesel exhibited the highest level of IVOC emissions
270 (784 ± 587 mg (kg fuel)$^{-1}$), followed by OGVs with MGO (651 ± 367 mg (kg fuel)$^{-1}$),
271 while OGVs with HFO showed the lowest levels (373 ± 218 mg (kg fuel)$^{-1}$). When it
272 came to SVOCs, ICSs with 0# diesel (1050 ± 817 mg (kg fuel)$^{-1}$) was still the highest,
273 followed by OGVs with MGO (530 ± 170 mg (kg fuel)$^{-1}$), and OGVs with HFO (509
274 ± 365 mg (kg fuel)$^{-1}$) still showed the lowest level. It could be seen that the switch of
275 fuels from HFO to MGO had enhanced both the emission of IVOCs and SVOCs.

276 Recently, IVOCs from ships have gained more and more attentions. The average
277 EF_{IVOCs} in this study exhibited a comparable yet slightly diminished level when
278 compared to previous on-board measurement results obtained from OGVs. For instance,
279 Huang et al. (2018a) quantified the IVOCs from an OGV and showed that the total
280 EF_{IVOCs} was 1003 mg (kg fuel)$^{-1}$. The average EF_{IVOCs} from low-sulfur fuel was 2.4
281 times higher than that from high-sulfur fuel. The IVOCs data measured from the same
282 tested OGVs in this study were also provided by Liu et al. (2022), revealing EF_{IVOCs} of
283 1830.5 and 1494.4 mg (kg fuel)$^{-1}$ for MGO and HFO, respectively. It is noting that the
284 EF_{IVOCs} measured in this study was lower compared with results from Liu et al. (2022),
285 which was mainly due to different analysis methods. The thermo desorption - gas
286 chromatography /mass spectrometry (TD-GC/MS) method was employed for the
287 analysis of IVOCs extracted from adsorption tubes in the study conducted by Liu et al.
288 (2022). While in order to maximize the identification of species, this study employed
289 organic solvent extraction coupled with BSTFA derivatization method; however, it is
290 important to note that this approach may potentially underestimate the total IVOCs.
291 Other studies also reported EF_{IVOCs} from different ship engines with different fuels. For
292 instance, Lou et al. (2019) conducted a study on the gaseous IVOCs emitted from a
293 main ship engine using HFO, and demonstrated that the EF_{IVOCs} ranged from 20.2 to
294 201 mg (kg fuel)$^{-1}$ on average. Moreover, Su et al. (2020) conducted a series of tests on
295 fuels of waste cooking oil (WCO) and MGO at the auxiliary engine test bench. They
296 found that the total EF_{IVOCs} of MGO and WCO were 2.33 ± 0.43 mg (kg fuel)$^{-1}$ and 1.47

297 ± 0.17 mg (kg fuel)$^{-1}$, respectively at the 75% of engine load. The findings from these
298 studies have demonstrated that the emission of IVOCs from ships can be influenced by
299 a multitude of influence factors, encompassing vessel types, fuel compositions, and
300 navigation conditions. However, limited research has been conducted on the
301 comprehensive emission factor of SVOCs and their constituents emitted from ships,
302 which also needs to gain more attention due to their non-negligible contribution to SOA
303 and O_3 formation (Robinson et al., 2007).

304 Figure 1 also illustrates the gas-particle partitioning of I/SVOCs from ship
305 exhausts in this study under low dilution ratios. Results showed that almost all I/SVOCs
306 in gas-phase had higher emission levels compared to particle-phase except for SVOCs
307 in HFO-ME. Previous studies focused on gaseous I/SVOC emissions of ship exhausts
308 and indicated that the gas-phase I/SVOCs played a crucial role in atmospheric chemical
309 reactions and aerosol formation processes (Liu et al., 2022;Lou et al., 2019). However,
310 the contribution of I/SVOCs from particles still could not be ignored. For example, the
311 contribution of particle-phase I/SVOCs to the total I/SVOCs could reach 16%-50% in
312 this study. Previous study has shown that they could continue to contribute to the
313 formation of SOA and O_3 largely through evaporation and oxidation in the atmosphere
314 (Drozd et al., 2021). Even though particle-phase reactions generally occur slower than
315 gas-phase reactions due to limitations imposed by oxidant diffusion and absorption into
316 aerosols (An et al., 2023), it still could be implied that particle-phase I/SVOCs were
317 similarly important precursors of SOA and O_3. The emissions of total I/SVOCs from
318 ships in both gas and particle phases should be thoroughly considered, as this could
319 potentially enhance the accuracy of simulation results for the formation of SOA and O_3.

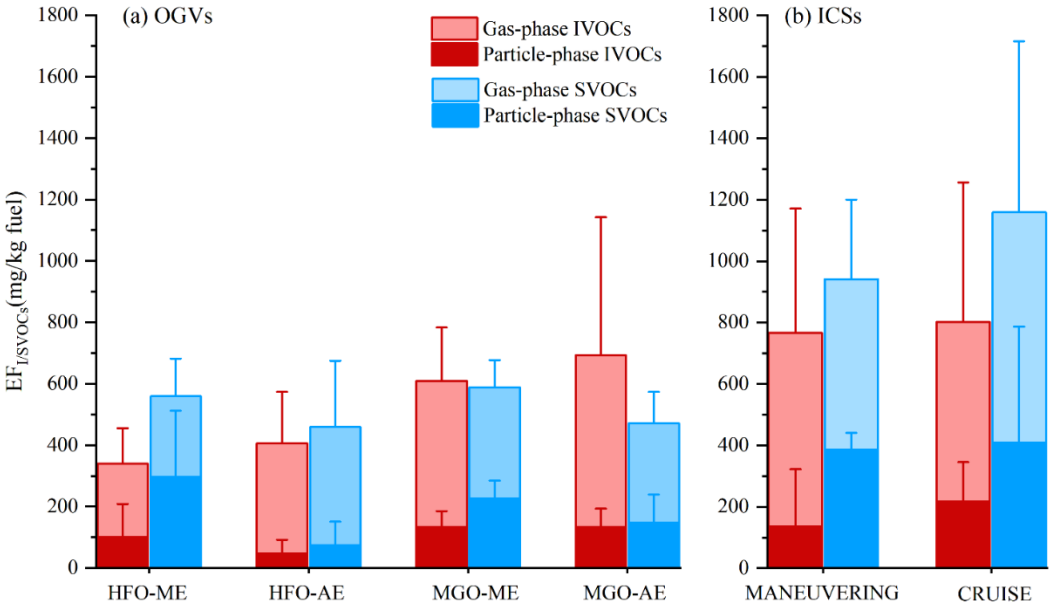

Figure 1 Emission factors of I/SVOCs in both gas-phase and particle-phase for OGVs and ICSs

3.2 Influence factors of I/SVOCs

The EFs for I/SVOCs emitted from ship exhausts exhibited significant variations under real-world conditions, as illustrated in Figure 1. In order to explore the impact of low sulfur fuel policy on I/SVOCs, $EF_{I/SVOCs}$ with different oil products (HFO, MGO, and 0# diesel) were given and discussed in this study (seen in Figure 2 (a)). Besides, $EF_{I/SVOCs}$ across diverse engine types (main engine (ME) and auxiliary engine (AE)), as well as various operating conditions (25%-90% operating modes of OGVs, cruise and maneuvering of ICSs) were also investigated (seen in Figure 2 (b) and (c)). Results showed that fuel type had considerable impact on the emission of I/SVOCs (Figure 2 (a)). $EF_{I/SVOCs}$ with 0# diesel presented the highest levels, followed by MGO, while HFO had the lowest $EF_{I/SVOCs}$. The mean $EF_{I/SVOCs}$ of 0# diesel, MGO, and HFO were 1834 ± 667, 1181 ± 421 and 881 ± 487 mg $(kg\ fuel)^{-1}$, respectively. The observation was noteworthy that a decrease in sulfur content of the fuel corresponded to an increase in $EF_{I/SVOCs}$ levels, as demonstrated by this study. Furthermore, relevant studies have also shown that the transition from high-sulfur to low-sulfur fuels resulted in an elevation of emission factors for both VOCs and IVOCs. For instance, Wu et al. (2020)

reported a 15-fold increase in EF_{VOCs} following the transition from high-sulfur (>0.5% m/m) to low-sulfur fuels, subsequent to the implementation of the low-sulfur policy. Zhang et al. (2021), Huang et al. (2018a) and Liu et al. (2022) also found negative correlations between sulfur content in fuel and IVOC emissions from ships. Study by An et al. (2023) in the Yangtze River Delta region found that both I/SVOCs and non-methane hydrocarbons (NMHCs) with low-sulfur oil had higher emission factors, which resulted in a high SOA formation potential. This meant that even though the use of lower sulfur content of fuels contributed to significant reduction in SO_x and PM emissions and mitigated their impact on environment. It also could lead to higher emissions of full-volatility organics during combustion, which had negative impacts on the formation of SOA and O_3 that further affected human health.

Fuel compositions could directly affect the emission characteristics of I/SVOCs. During the combustion of fuel, the generation of I/SVOCs could involve complex processes, such as pyrolysis of organic matters, dehydrogenation, oxygenation and incomplete combustion (Akherati et al., 2019;Zhao et al., 2014). A large portion of I/SVOCs derived directly from incomplete combustion of fuel (Zhang et al., 2016;Liu et al., 2022). The main components of 0# diesel are typically hydrocarbons, including alkanes, cycloalkanes, and aromatic hydrocarbons. These components are mostly within the range of I/SVOCs, mainly composed of complex hydrocarbons ranging from C_{12} to C_{22} (Alam et al., 2018). The similar compositions of 0# diesel to I/SVOCs might be the primary reason for its highest emission levels. MGO and HFO both belong to marine fuel oil (Corbin et al., 2018). MGO is a kind of light marine diesel, while HFO refers to the black, viscous residue left after distilling lighter fractions such as gasoline, kerosene, and diesel from crude oil, or a blend of the black, viscous residue with lighter fractions (Schüppel and Gräbner, 2024). HFO are categorized into HSF and low-sulfur fuel (LSF). HSF were generally utilized before low-sulfur standards were introduced, while LSF have been adopted since these standards were enacted, enabling compliance

with stricter environmental regulations through reduced sulfur content. Unless otherwise specified, HFO in this study refers to LSF-HFO. Referred to the measured organic compositions of MGO and HFO from Liu et al. (2022), it could be seen that MGO had higher n-alkanes but lower PAHs compared with HFO. This was also one main reason for the higher $EF_{I/SVOCs}$ for MGO than HFO. Moreover, sulfides play a catalytic role in combustion, reducing the ignition temperature of the fuel (Ju and Jeon, 2022). The ignition point of low-sulfur fuel is comparatively higher than that of high-sulfur fuel, thereby necessitating elevated temperatures and increased oxygen input to achieve complete combustion (Dinamarca et al., 2014;Drozd et al., 2019). Therefore, the incomplete combustion might be enhanced for low-sulfur fuel at similar engine loads (Zhao et al., 2015), leading to greater production of I/SVOCs for low-sulfur fuel. To further elucidate the impact of reduced sulfur content on combustion efficiency, we calculated the modified combustion efficiencies (MCE) for various fuel types (Figure S2). The results indicated a notable decline in MCE values as the sulfur content decreased, suggesting that incomplete combustion was a key factor contributing to the elevated levels of I/SVOCs in low-sulfur fuels.

The operating condition was another important factor that affected ship I/SVOCs emissions. During actual navigation of OGVs, the operating modes were ranging from engine load of 25% to 90%. In this study, the operating modes were categorized into three distinct levels: low mode for engine loads below 50%, medium mode for loads between 50% and 75%, and high mode for loads exceeding 75%. As for the ICSs, because the time for departure and docking could be neglected compared with long-distance cargo transportation, cruise and maneuvering were selected according to the actual operating conditions. The engine operating load was higher in cruise mode (classified as high mode) compared with maneuvering (medium mode). ~~It could be seen from Figure 2 (b) that (Zhao et al., 2014;Huang et al., 2018b). Operating modes affect the combustion state in engines the air-fuel ratio during the combustion process, thereby influencing exhaust emissions (Shrivastava and Nath Verma, 2020). Poor mixing state~~

~~of air and fuel at low loads leads to decreased temperature and pressure during fuel combustion (Zhao et al., 2021), which in turn leads to incomplete combustion of fuel. The high operating mode is associated with reduced fuel diffusion and combustion time, leading to a partial oxygen deficiency within the cylinder, thereby resulting in an increased generation of I/SVOCs (Zhao et al., 2016;Liu et al., 2022). The investigation of methodologies for optimizing engine design and control systems to achieve enhanced combustion efficiency under operating conditions, thus reducing emissions, is of great significance.~~It could be seen from Figure 2 (b) that the average emission factors (EFs) of I/SVOCs in this study followed a relatively ascending order across operating modes: 1098 ± 305 mg $(kg\ fuel)^{-1}$ in low, 1542 ± 465 mg $(kg\ fuel)^{-1}$ in medium and 1457 ± 276 mg $(kg\ fuel)^{-1}$ in high operating modes, respectively in this study, revealing significantly elevated emissions at both medium and high loads compared to low-load conditions. This trend was consistent with PM emission patterns reported by Zhang et al. (2021), but notably diverged from the characteristics of ship-emitted IVOCs, which reached its lowest value under medium-load conditions in prior studies (Zhao et al., 2014;Huang et al., 2018b). This discrepancy could be attributed to the dominance of SVOCs over IVOCs in this study. Operating modes affect the combustion state in engines and the air-fuel ratio during the combustion process, thereby influencing exhaust emissions (Shrivastava and Nath Verma, 2020). The air-fuel ratio exhibits a decreasing trend with increasing engine load, which induces more pronounced incomplete combustion within the cylinder, thereby establishing a direct causative relationship with elevated total I/SVOC emissions. (Zhang et al., 2021; Watson et al., 1994). The high operating mode is associated with reduced fuel diffusion and combustion time, leading to a partial oxygen deficiency within the cylinder, thereby resulting in an increased generation of I/SVOCs (Zhao et al., 2016;Liu et al., 2022). The investigation of methodologies for optimizing engine design and control systems to achieve enhanced combustion efficiency under different operating conditions, thus reducing emissions, is of great significance.

Engine type also led to difference of I/SVOC emissions from ships. There were two types of engines on the OGVs, which were low-speed engines (LSE) for the main engines (ME) and medium-speed engines (MSE) for the auxiliary engines (AE). While only one type engine on the ICSs as the main engines, which were high-speed engines (HSE) (seen in Table S1). The findings indicated that there were no statistically significant differences in the $EF_{I/SVOCs}$ among various engines. Typically, medium-speed engines exhibit lower combustion efficiencies than low-speed engines, leading to higher I/SVOC emissions (Wu et al., 2020;Liu et al., 2022). However, because as AEs, the MSEs used in this study were almost operated in medium loads that always presented the lowest pollutants as described above, which resulted in the lowest I/SVOC emissions as well. This finding suggested that the influence of operating conditions offset that of engine type, ultimately resulting in similar levels of EFI/SVOCs for the MSE compared to the LSE. $EF_{I/SVOCs}$ for ICSs with high-speed engines presented the highest level (1370 ± 382 mg (kg fuel)$^{-1}$). As previously mentioned, high-speed engines typically exhibit lower combustion efficiencies compared to other engine types (Wu et al., 2020), while the utilization of low-sulfur fuel also results in elevated levels of $EF_{I/SVOCs}$. Therefore, both the engine type and fuel type used for ICSs jointly caused the highest $EF_{I/SVOCs}$ in this study. In summary, fuel types determine emission compositions, while engine type and operating conditions affect combustion efficiency and reaction paths. These factors interact, thereby leading to varying degrees of incomplete combustion, ultimately resulting in complex I/SVOCs emissions.

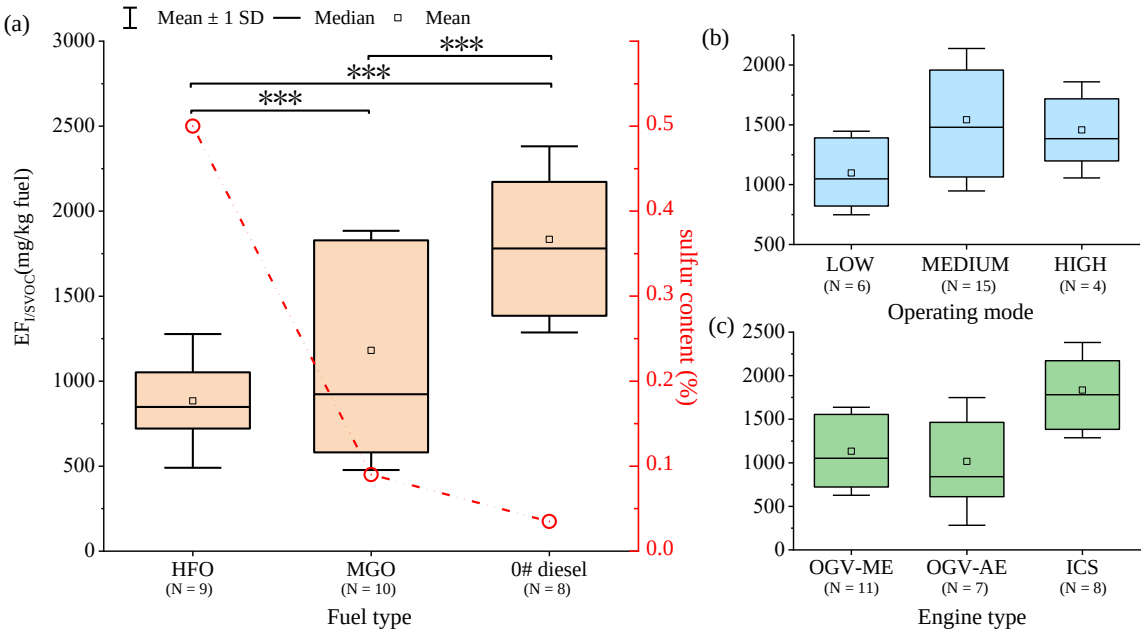

Figure 2 Box-whisker plots of total $EF_{I/SVOCs}$ for the tested ships under (a) different fuel types, (b) different operating modes, and (c) different engine types. N represents the number of samples. Significant differences between samples were determined using an independent samples T-test. The error bars represent the standard deviation of the measured values, while *** indicates a significance level of $p < 0.001$.

3.3 Chemical compositions and profiles of I/SVOCs

3.3.1 Chemical compositions of I/SVOCs

The chemical compositions (speciated I/SVOCs and UCM) of I/SVOCs emitted from OGVs and ICSs under various operating conditions are presented in Figure 3. The speciated I/SVOCs included n-alkanes, branched alkanes (b-alkanes), (O)PAHs, hopanes and acids. In general, UCM and b-alkanes dominated the total I/SVOCs from ship exhausts, contributing 83.4% to 89.8% of the total I/SVOCs (speciated + UCMs). The emissions of acids and n-alkanes were also noteworthy, accounting for an average of 6.51% and 4.61% of the total I/SVOCs, respectively. Previous studies also have noted the relatively high proportion of n-alkanes in I/SVOCs from shipping emission sources (Huang et al., 2018a;He et al., 2022a). However, there is limited data available on organic acids, particularly those emitted by shipping activities. PAHs, hopanes, and benzoic acids collectively contribute only about 1% to the overall emissions, indicating their relatively minor role. However, even though these substances only constituted a

small proportion of the overall emissions, the environmental and health effects still demanded in-depth research and vigilance due to their strong toxicity and bio-accumulative nature (He et al., 2022b;Mochida et al., 2003).

It is noteworthy that both the EFs and proportions of fatty acids in the total I/SVOCs were found to be remarkably high in this study, as previously mentioned. This finding aligns with the results reported by Huang et al. (2018a) and Wang et al. (2023), where n-fatty acids were identified as a significant component of chemical compositions derived from an OGV exhaust. However, there is still very little research on fatty acids from shipping emissions. Fatty acids are a category of organic compounds with carboxyl groups and relatively long carbon chains, playing essential physiological roles within organisms. Prolonged exposure to elevated levels of fatty acid pollutants has been linked to the development of respiratory, immune, and cardiovascular disorders (He et al., 2022a;He et al., 2022b). Studies have indicated that fatty acids can constitute a substantial portion of the organic matter in atmospheric aerosols, especially in marine aerosols (Hu et al., 2023;Mochida et al., 2003;Kawamura et al., 2017). For example, research in the North Pacific had shown that fatty acids could account for 10% to 30% of organic carbon (Mochida et al., 2003;Mochida et al., 2002). In addition, low-molecular-weight fatty acids ($C_{14:0}$-$C_{19:0}$) have been increasing in the North Pacific in recent years (Hu et al., 2023). The content of fatty acids in marine aerosols was relatively high, yet their specific sources were often attributed to biomass burning and biological emissions in the past (Hu et al., 2023;Kawamura et al., 2010). It could be inferred from the results in this study that shipping emission might be one significant potential contributor to the fatty acids in marine aerosols. Besides, the EF of fatty acids were found to be higher in ship exhausts fueled by MGO and 0# diesel compared to HFO, which aligns with the findings of Huang et al. (2018a) indicating that the average EF of n-fatty acids from LSF was 6.7 times greater than that from HSF. Consequently, the forthcoming implementation of a globally uniform ultra-low-sulfur oil policy may potentially lead to an elevated release of fatty acids, particularly in coastal and inland

regions. Given studies on acid pollutants from ship exhausts were relatively scarce or they had been overlooked due to limitations in sampling and detection methods, further investigation is warranted to enhance the comprehension of the characteristics and influences of acidic emissions derived from ship exhausts.

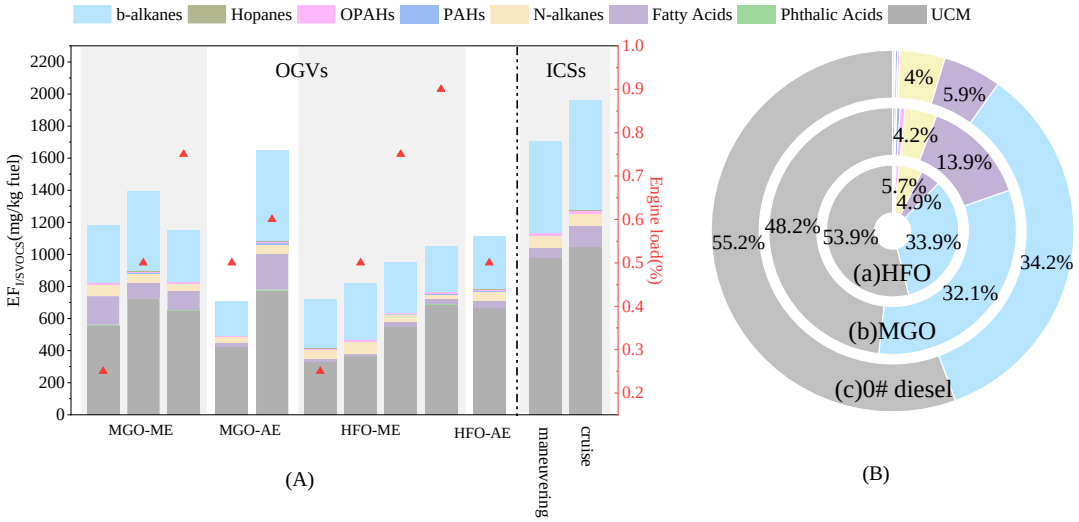

Figure 3 Chemical compositions of I/SVOCs from the tested ships, (A) emission factors (mg (kg fuel)$^{-1}$) and (B) fractional contributions (%). The red triangles represent the engine load.

As mentioned above, the total $EF_{I/SVOCs}$ of ship exhausts was significantly influenced by fuel type. The average emission factors of the primary chemical compositions of I/SVOCs under various fuel conditions are presented in Table 2. Results demonstrated that the EFs of the majority of organic compounds in ship emissions exhibited an upward trend as the sulfur content in fuels decreased. Specifically, emission factors of UCM, branched alkanes and (O)PAHs for 0# diesel were much higher than the other two fuels, with HFO having the lowest values. While in terms of n-alkanes, the average total EFs of n-alkanes in these fuel types were 72.9 ± 28.1 mg (kg fuel)$^{-1}$(0# diesel), 50.1 ± 15.1 mg (kg fuel)$^{-1}$(HFO) and 49.2 ± 11.2 mg (kg fuel)$^{-1}$(MGO), respectively, indicating a slight deviation from the findings of Liu et al. (2022) regarding the higher $EF_{n\text{-alkanes}}$ in MGO compared to HFO. This might be explained by that not only n-alkanes in IVOCs, but also SVOCs were detected in this study. Compared with IVOCs referring from C_{12} to C_{22}, SVOCs (C_{22}-C_{36}) from HFO

had higher emission factor values due to the higher carbon chains than MGO (details also have been shown in Section 3.4), which offset the higher $EF_{n\text{-alkanes}}$ caused by IVOCs (seen in Figure 1). Besides, compared with the other two types of fuels, MGO emitted higher emission factor level of acids. MGO is a blend of straight-run light distillate diesel and secondary processed diesel from crude oil (Ahn et al., 2021), which may contain a considerable amount of impurities, which could be a reason for its higher content of acidic substances. However, hopanes from HFO presented the highest emission factor level, which was one rare category of organic matters that decreased with the improvement of fuel quality. The details will be discussed in Section 3.3.2.

Table 2 Average emission factors of main chemical compositions of I/SVOCs under different fuels (mg (kg fuel)$^{-1}$)).

Fuel Type	UCM	B-alkanes	Acids	N-alkanes	(O)PAHs	Hopanes
HFO	492±137	299±17.5	27.7±10.6	50.1±15.1	9.47±3.1	2.99±1.01
MGO	608±109	379±112	129±57.7	49.2±11.2	12.9±5.3	2.41±0.88
0# diesel	1010±134	628±55.7	99.5±33.9	72.9±28.1	21.4±3.3	1.88±0.82

3.3.2 Profiles of I/SVOCs

Detailed profiles of organic compounds from ship exhausts are of great significance for source identification. The profile characteristics of the identified organic compounds, including fatty acids, n-alkanes, PAHs, OPAHs, and hopanes measured from the three types of ships in this study are presented in Figure 4. Results showed that fatty acids with 11-18 carbon numbers ($C_{11:0\text{-}18:0}$ and $C_{18:1}$) were the main acids emitted from ships, especially *n*-C_{14} and *n*-C_{18}. In addition, it showed that HFO had a significantly lower proportion of Dodecanoic ($C_{12:0}$) and Tetradecanoic ($C_{14:0}$) compared with 0# diesel and MGO, while the proportion of Octadecanoic ($C_{18:0}$) in 0# diesel was lower than other fuels. The $C_{18:0}$ to $C_{14:0}$ ratios of HFO, MGO and 0# diesel were 3.7 ± 1.0, 0.3 ± 0.2 and 0.1 ± 0.4, respectively. This $C_{18:0}$ to $C_{14:0}$ ratio decreased significantly with the decrease of sulfur content of the fuel. Besides, the average proportion of fatty acids containing an even number of carbons (88.05% ± 3.7%) in this study was significantly higher than that of fatty acids with an odd number of carbons.

Previous studies have demonstrated a robust distribution of fatty acids with even-numbered carbon chains in marine aerosols, exhibiting distinct peaks at *n*-C_{16} and *n*-C_{18} (Hu et al., 2023;Kawamura et al., 2017;Mochida et al., 2002), thereby providing further evidence that ship exhaust emissions constitute a significant source of fatty acids in marine aerosols. Given the limited availability of studies on single-source acids, it is imperative to gather additional evidence regarding acid pollution resulting from ship transportation emissions. This will enhance our comprehension of the magnitude of the issue and the environmental and human health implications associated with these emissions.

The n-alkane profiles of the three types of fuels in this study (depicted in Figure 4) clearly indicated that low carbon number n-alkanes exhibit dominance. N-nonadecane (C_{19}) was the highest compositions for both HFO and MGO. While 0# diesel exhibited a peak at heptadecane (C_{17}), which was mainly caused by the characteristic of fuel compositions. Significant variations were observed in the emissions of n-alkanes from other non-internal combustion engine sources, such as high composition of n-octacosane (C_{29}) and apparent odd-carbon advantages in biomass emissions (Hu et al., 2023;Perrone et al., 2014); high compositions in C_{23} and C_{21} for coal combustion (Duan et al., 2010;Xie et al., 2009).

The PAH profiles associated with different fuel types in this study exhibited similar patterns to those observed by Liu et al. (2022), wherein low molecular weight PAHs were found to constitute a relatively higher proportion. The major compounds in this study were Phenanthrene (Phe), Pyrene (Pyr), Fluorene (Flu), Chrysene (Chr) and Benzo[a]pyrene (Bap), aligning with the conclusions of previous studies (Zhang et al., 2016;Zhang et al., 2014). PAHs from 0# diesel had higher proportion of Pyr and lower proportion of Bap compared with the other two types of fuels. Besides, high proportions of 1-Naphthaldehyd (1-Nap) and Anthraquinone (ATQ) in OPAHs were also revealed from ship exhausts in this study, with 1-NAP for 0# diesel having the highest level. Most of the PAHs and OPAHs emitted in this study were low molecular weight tricyclic

and tetracyclic substances, accounting for 94.7% to 96.9% of total OPAHs + PAHs, and 6.6%±2.1%, 6.7%±1.7% and 10.1%±5.9% of the total speciated I/SVOC profile in HFO, MGO and 0# diesel, respectively. The present study observed a positive correlation between the decrease in sulfur content and an increase in OPAHs + PAHs with smaller ring numbers emitted from ship exhausts, while conversely, higher ring compounds exhibited a negative relationship. Specifically, 1-Nap accounted for significantly higher proportion of OPAHs + PAHs in 0# diesel (70.4% ± 1.2%) than in MGO (47.9% ± 7.3%) and HFO (36.6% ± 15.2%). As the sulfur content decreased, both the emission factor level and proportion of 1-NAP exhibited an increasing trend.

Hopanes are found mainly in coal, fuel oils and lubricants and are generally regarded as molecular markers of fossil fuel combustion sources due to their stable chemical property (Cass, 1998). In this study, C_{29ab} and C_{30ab} were the main hopanes emitted from ships, accounting for 67.1% ± 5.5% of the total hopanes. In addition, $C_{31ab\ S}$, $C_{31ab\ R}$ and $C_{32ab\ S}$ also showed non-ignorable contributions in ship emissions. Different from n-alkanes and (O)PAHs, among the fuels, hopanes presented the highest proportions from exhausts of HFO, followed by MGO, while 0# diesel showed the lowest levels. This finding was consistent with the results reported by Sippula et al. (2014), which demonstrated that HFO operation yields higher concentrations of hopanes compared to diesel fuel. The primary reason for this disparity was attributed to the presence of hopanes in HFO, whereas lubrication oil served as the sole source of these compounds during diesel fuel operation (Kleeman et al., 2008). Given vanadium and nickel cannot continue to be typical tracers of ship exhausts with low-sulfur content HFO (Yu et al., 2021), organic diagnostic characteristics such as hopanes coupled with the ratio of $C_{18:0}$ to $C_{14:0}$ could be considered as potential markers of HFO exhausts.

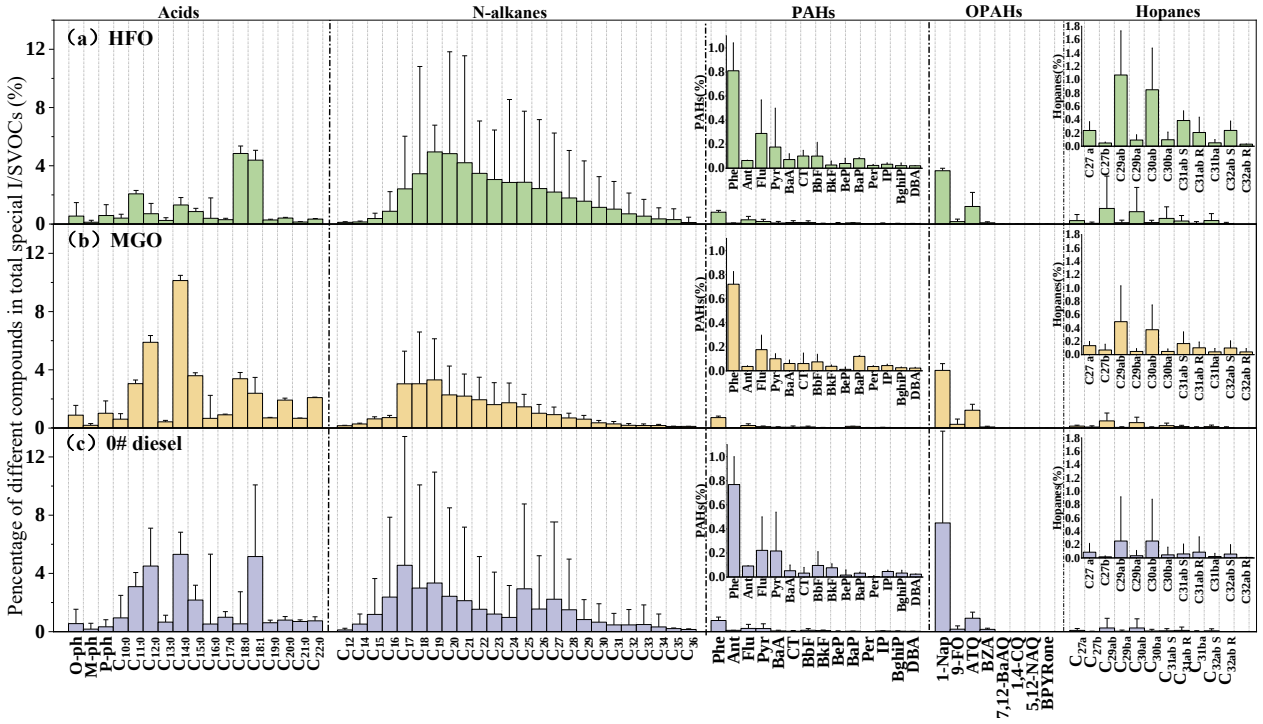

Figure 4 Profiles of I/SVOCs in ship exhausts under different fuels

3.4 Volatility Distribution of I/SVOCs

Volatility distribution of I/SVOCs from ships is shown in Figure 5, 24 Bins were divided using n-alkanes as an indicator. What needs to illustrate was that the effective saturation concentration (C*) of n-alkanes in each bin was used as a surrogate value to discuss the volatility distribution of I/SVOCs (Zhao et al., 2016;Zhao et al., 2014). The employed experimental method of solvent extraction in this study should be acknowledged for its potential to underestimate highly volatile organic compounds. However, in the meantime, this method could also effectively identify and quantify as many I/SVOC species as possible. Figure 5 shows the proportion of I/SVOCs in each volatile bin to further investigate the effects of different factors on I/SVOCs. Obviously, fuel type had apparent impact on the overall trend of volatility distribution of $EF_{I/SVOC}$, with similar volatility profiles of identical fuels (Figure 5 (a)). While operating mode and engine type also affected the volatility distributions of I/SVOCs (Figure 5 (b)). For example, for both HFO-ME and MGO-ME of OGVs, there were maximum values in bin 29. The range and

magnitude of this maximum region increased with engine load, reaching its peak at 50% engine load and subsequently declining at 75% engine load (Figure 5 (b)). The higher emissions of I/SVOCs in low-speed and high-speed loads might be significantly influenced by the increase of these low-volatile components.

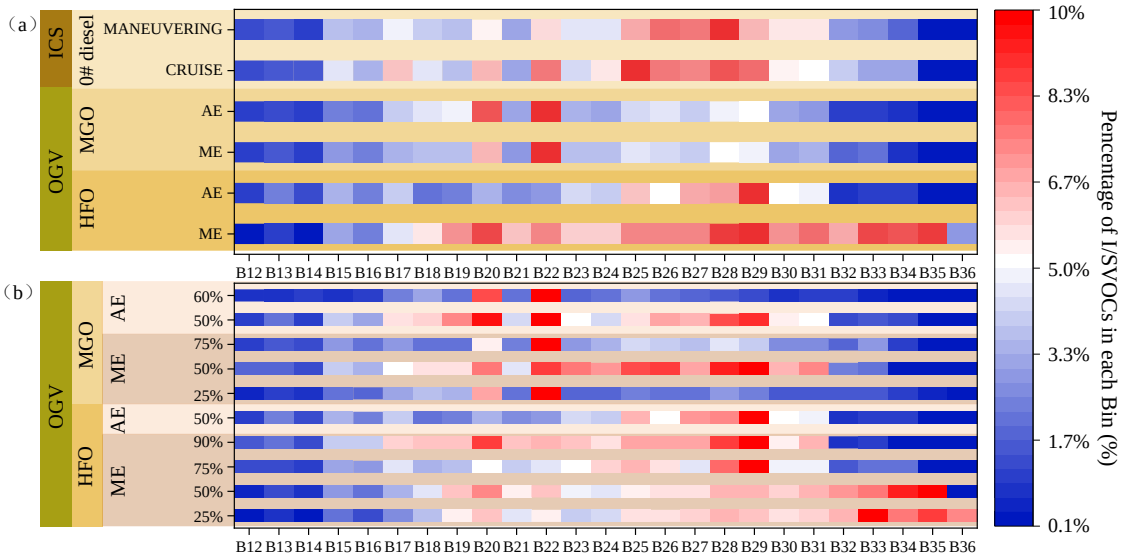

Figure 5 Split-bar heat plot of the I/SVOCs proportions in each volatile bin under (a) different fuel types for different engines, and (b) different operating conditions (25%-90% operating modes) for OGVs

In order to figure out the volatility distributions of detailed chemical compositions of I/SVOCs from different fuels. The average volatility distributions of UCM, b-alkanes, n-alkanes, PAHs, acids and hopanes based on the volatility basis set (VBS) framework are given in Figure 6. Results revealed that the volatility distributions of UCM exhibited distinct bimodal characteristics, with peak values occurring at log C* = -3 to -2 and log C* = 3 to 4. Notably, the concentration was more pronounced in the low-volatility region. Moreover, the bimodal characteristic of UCM in 0# diesel was more pronounced compared to HFO and MGO. Additionally, HFO exhibited a higher proportion of low-volatility UCM relative to 0# diesel and MGO. The volatile distributions of n-alkanes exhibited a bimodal structure, with peaks occurring at log C* = -4 to -2 and log C* = 5 to 6, respectively. Furthermore, from HFO to MGO and finally to 0# diesel, the VBS

peak of n-alkanes progressively shifted towards the higher volatility range. This shift could be attributed to the distinct characteristics of these fuels, where MGO and 0# diesel had lower boiling points and contained fewer carbon atoms in their hydrocarbon chains compared to HFO (Liu et al., 2022). The volatility distributions of other specific I/SVOCs were consistent with their molecular sizes. (O)PAHs emitted from ships were predominantly small molecules with high volatility, primarily enriched in the log C* range of 4 to 5. Acids were mainly concentrated in the higher volatility bins (log C* = 0 to 5), whereas hopanes exhibited a primary concentration in the lower volatility intervals. The compositions and physicochemical properties of different fuel types vary, leading to differences in the volatile organic compounds they contain. Consequently, the type of fuel played a significant role in determining the distribution of volatile fractions for each individual I/SVOC component. The composition and combustion efficiency of fuel are important factors affecting the emission and distribution of I/SVOCs.

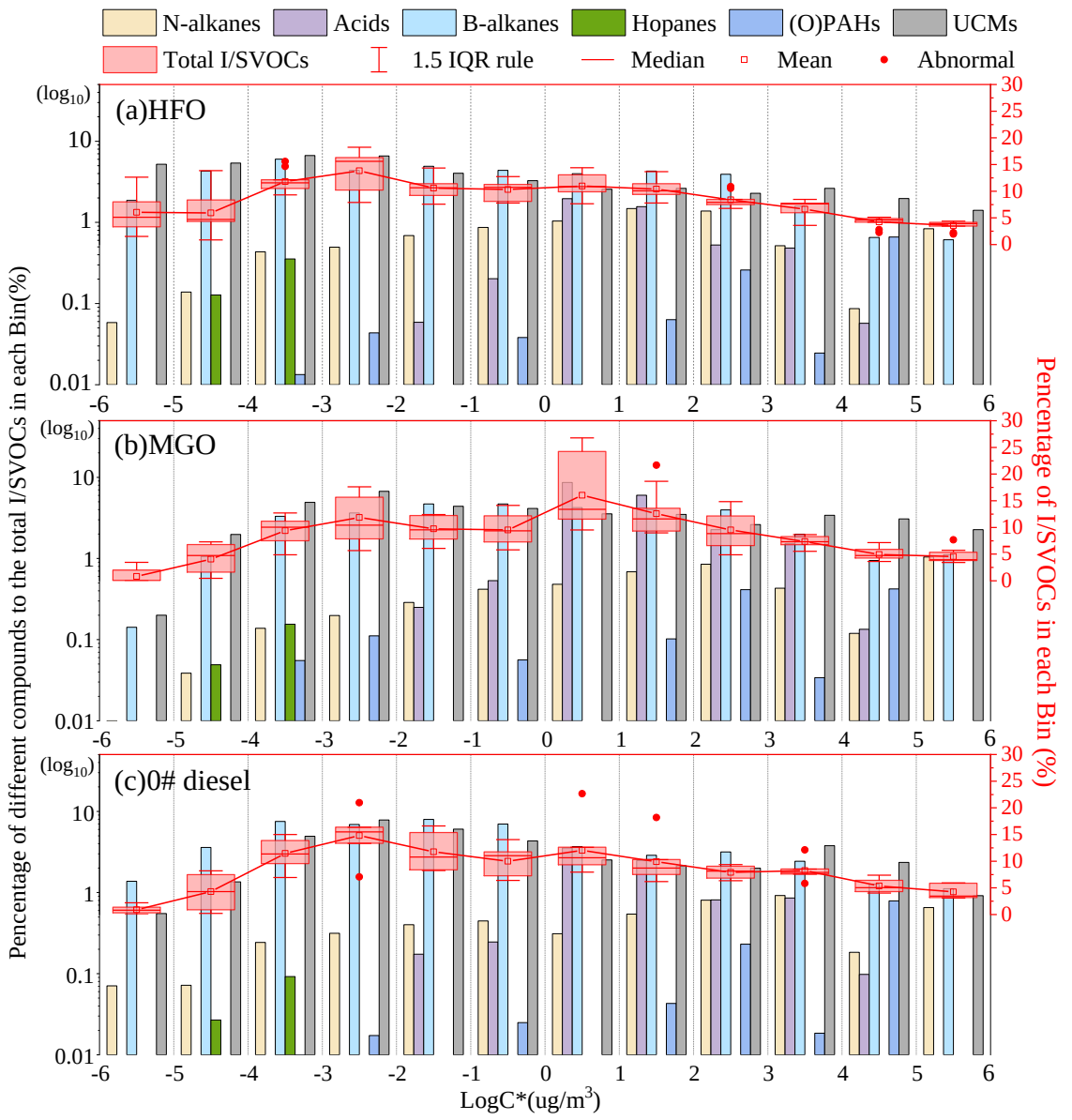
N-alkanes
Acids
B-alkanes
Hopanes
(O)PAHs
UCMs
Total I/SVOCs
1.5 IQR rule
Median
Mean
Abnormal
(a)HFO
(b)MGO
(c)0# diesel
(log10)
Pencentage of different compounds to the total I/SVOCs in each Bin(%)
Pencentage of I/SVOCs in each Bin (%)
LogC*(ug/m3)

642

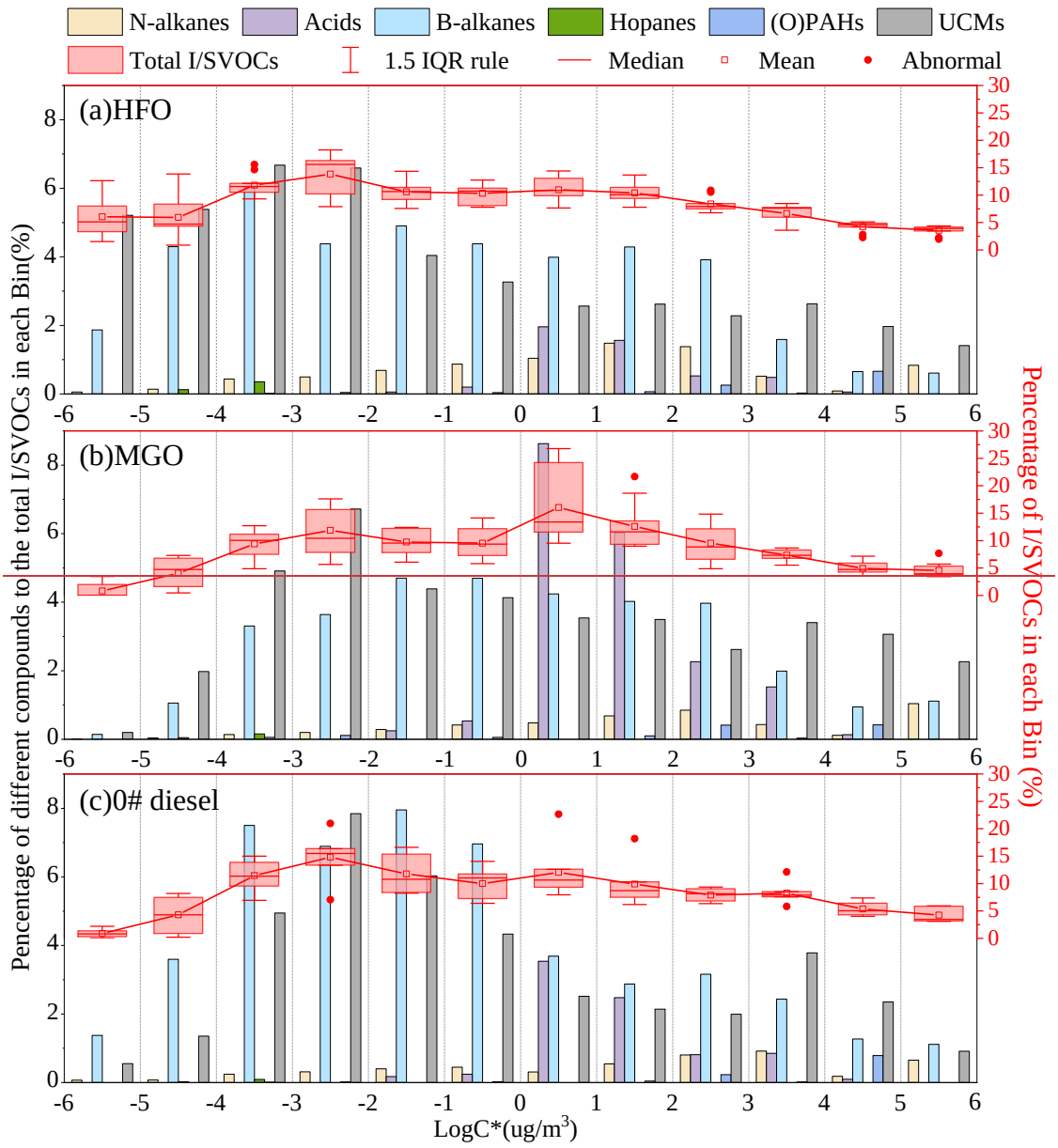

Figure 6 The volatility distributions of I/SVOCs based on the volatility basis set (VBS) framework from different fuels

3.5 SOA formation potential of I/SVOCs

I/SVOCs have been proposed as crucial precursors of SOA (Murphy et al., 2017;Hu et al., 2023). However, most of previous studies about ship exhausts focus on the contribution of gas-phase IVOCs on SOA (Huang et al., 2018b;Liu et al., 2022), the contributions from IVOCs and SVOCs in particle-phase have been neglected. The comprehensive assessment of ship exhaust emissions, encompassing both gas-phase and particle-phase I/SVOCs, was crucial for evaluating the overall impact on the environment. This became particularly important in light of the implementation of low-

sulfur fuel policies, which had resulted in increased emissions of full-volatility organic compounds. Therefore, the SOAFPs of I/SVOCs from ships with different fuels were estimated (shown in Figure 7). Results showed that in terms of the total SOAFP evaluated from both IVOCs and SVOCs, 0# diesel and MGO with the lower sulfur content showed higher values, which could reach as high as 634 mg (kg fuel)$^{-1}$ and 418 mg (kg fuel)$^{-1}$, respectively. In comparison, the SOAFP from HFO only had a lower value of 354 mg (kg fuel)$^{-1}$. For IVOCs, the use of low-sulfur 0# diesel and MGO could lead to higher SOAFP that reached 234 mg (kg fuel)$^{-1}$ and 157 mg (kg fuel)$^{-1}$ respectively, while HFO exhibited a significantly lower SOAFP level of only 101 mg (kg fuel)$^{-1}$. As for SVOCs, the SOAFPs of those three fuels were 400 mg (kg fuel)$^{-1}$ for 0# diesel, 261 mg (kg fuel)$^{-1}$ for MGO and 253 mg (kg fuel)$^{-1}$ for HFO. Previously, there has been limited research on SVOCs and their SOAFP, resulting in a scarcity of relevant comparative studies. Compared to diesel vehicles (430 ± 574 mg (kg fuel)$^{-1}$), gasoline vehicles (39 ± 79 mg (kg fuel)$^{-1}$) and ~~N~~nonroad machinery (424 ± 138 mg (kg fuel)$^{-1}$) reported in previous IVOC studies (Zhao et al., 2015; Zhao et al., 2016;Qi et al., 2019), SOA emissions of total I/SVOCs from ships using 0# diesel exhibit significantly higher formation potential (634 mg (kg fuel)$^{-1}$)~~-~~. This discrepancy highlights critical knowledge gaps in current assessments, where the scarcity of research on SVOCs and their SOAFP has led to incomplete comparisons. Results from this study indicated that SOAFP could be enhanced with the decrease of sulfur content, the same as I/SVOCs emission factors. The major contribution to the total SOAFPs was observed from B-alkanes and UCM, accounting for 81.1%-87.8%, while the significance of acids, particularly IVOCs, should not be overlooked. Besides, SOAFPs from SVOCs were higher than that of IVOCs, no matter what types of fuels, which further indicated the importance of SVOCs. However, due the analysis method of I/SVOCs, the emission factor as well as SOAFP were underestimated in this study. More real-world measurement of chemically identifiable full-volatility organic matters should be carried out to figure out their emission characteristics and SOAFPs, especially for the ultra-

low-sulfur marine fuels, which could provide basis for the further establishment of ship emission policies.

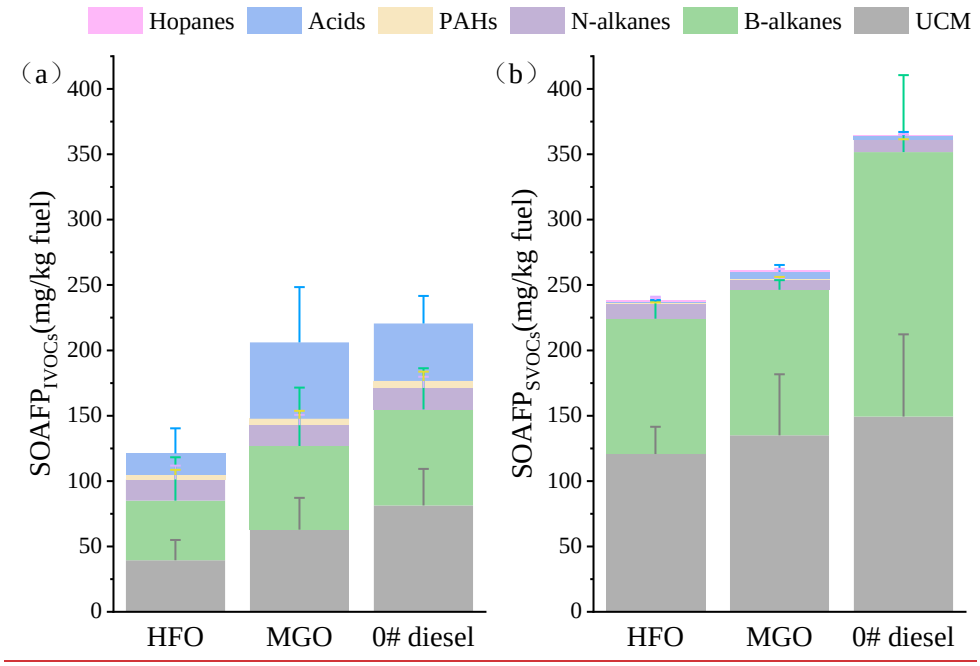

Figure 7. SOAFP from (a) IVOCs and (b) SVOCs.

4 Conclusions and atmospheric implications

The results revealed that $EF_{I/SVOCs}$ of ICSs were higher than OGVs. Furthermore, a decreasing sulfur content in fuel was found to be associated with an increasing trend in $EF_{I/SVOCs}$. Fuel quality, engine type, and engine load all exerted significant influences on the emissions, compositions, and volatility distributions of I/SVOCs. Besides, the most predominant I/SVOC components were UCM and b-alkanes, followed by acids and n-alkanes. Notably, a significant presence of fatty acids was detected in ship exhausts, warranting further attention, particularly towards fatty acids ranging from C_{11}-C_{18} carbon numbers. It also found that organic diagnostic markers of hopanes, in conjunction with the $C_{18:0}$ to $C_{14:0}$ acid ratio, could be considered as potential markers for HFO exhausts. Moreover, the transition from low-sulfur content to ultra-low-sulfur content fuels had also enhanced the secondary organic aerosol formation potential.

The findings of this study, along with previous research, suggest that a decrease in sulfur content in fuels leads to a significant increase in emissions of full-volatility organics from OGVs. This further exacerbates the SOAFP, which pose serious

environmental and health risks, particularly in densely populated coastal areas. Therefore, there is a need for optimization of the implementation of an ultra-low-sulfur oil policy. Due to data limitations, previous emission inventories for ships often underestimated the emissions of organic matter, particularly from I/SVOCs. This underestimation has led to an incomplete assessment of the contribution of ship emissions to air quality, particularly in terms of SOA formation. Specifically, according to existing emission inventories based on previous studies, the total IVOCs emissions from non-road mobile sources amount to 238 Gg, with ships contributing 6.16% (14.7 Gg) of this total (Zhao et al., 2022). Assuming these ships use low-sulfur fuel (with a sulfur content of below 0.5% (m/m)) and applying the emission factors from this study for re-estimation, the unconsidered SVOCs would lead to an underestimation of 11.9 Gg pollutant emissions. If the sulfur content of the fuel is further reduced to 0.1% ultra-low sulfur fuel oil (with a sulfur content of below 0.1% (m/m)), the revised IVOCs emissions from ships would be 17.7 Gg, and SVOCs emissions would be 23.6 Gg, representing a 64% increase in total emissions compared to using low-sulfur fuel.

–Moreover, high proportions of acidic substances in I/SVOCs from ships were found in this study, which extended the profiles of ship exhaust emissions. It also could be inferred that organic diagnostic characteristics, such as hopanes, in combination with the ratio of $C_{18:0}$ to $C_{14:0}$ could be considered as potential markers for HFO exhausts. However, there were still limitations in this study that the experimental method used might lead to the underestimation of highly volatile organic compounds. –Besides, more than half of the I/SVOCs still could not be identified in this study. –Improved experimental method needs to be considered to identify more full-volatility organic substances with greater precision and accuracy in future study. Future research can obtain more comprehensive and accurate organic component emission data by using advanced methods such as comprehensive two-dimensional gas chromatography-mass spectrometry (GC × GC-MS) and Orbitrap mass spectrometry. Considering the proven effectiveness of after-treatment systems, such as diesel oxidation catalyst (DOC), diesel

particulate filter (DPF), and selective catalytic reduction (SCR), in reducing emissions of full-volatility organic compounds (Reşitoğlu et al., 2015;Nadanakumar et al., 2021;Biswas et al., 2009;Yashnik and Ismagilov, 2023;Hamada and Haneda, 2012), these systems could be regarded as potential measures to mitigate the elevated levels of I/SVOCs emitted by ships.

Author contributions:

FZ, GW, YZ, and YC conceptualized and designed the study; BX, ZL, XW, YW, YH, MC, and YbC performed the measurements; FZ, RL, CW, LZ, and GW analyzed the data. BX wrote the manuscript draft; All the authors reviewed, edited, and contributed to the scientific discussion in the manuscript.

Competing interests

The contact author has declared that none of the authors has any competing interests.

Acknowledgments

This study was supported by the National Natural Science Foundation of China (42377096, 42130704, U23A2030).

References

Ahn, S., Seo, J. M., and Lee, H.: Thermogravimetric Analysis of Marine Gas Oil in Lubricating Oil, J. Mar. Sci. Eng., 9, 339, 2021.

Akherati, A., Cappa, C. D., Kleeman, M. J., Docherty, K. S., Jimenez, J. L., Griffith, S. M., Dusanter, S., Stevens, P. S., and Jathar, S. H.: Simulating secondary organic aerosol in a regional air quality model using the statistical oxidation model – Part 3: Assessing the influence of semi-volatile and intermediate-volatility organic compounds and NO_x, Atmos. Chem. Phys., 19, 4561-4594, 10.5194/acp-19-4561-2019, 2019.

Alam, M. S., Zeraati-Rezaei, S., Liang, Z., Stark, C., Xu, H., MacKenzie, A. R., and Harrison, R. M.: Mapping and quantifying isomer sets of hydrocarbons($\geq C_{12}$) in diesel exhaust, lubricating oil and diesel fuel samples using GC × GC-ToF-MS, Atmos. Meas. Tech., 11, 3047-3058, 10.5194/amt-11-3047-2018, 2018.

An, J., Huang, C., Huang, D., Qin, M., Liu, H., Yan, R., Qiao, L., Zhou, M., Li, Y., Zhu, S., Wang, Q., and Wang, H.: Sources of organic aerosols in eastern China: a modeling study with high-resolution intermediate-volatility and semivolatile organic compound emissions, Atmos. Chem. Phys., 23, 323-344, 10.5194/acp-23-323-2023, 2023.

Biswas, S., Verma, V., Schauer, J. J., and Sioutas, C.: Chemical speciation of PM emissions from heavy-duty diesel vehicles equipped with diesel particulate filter (DPF)

766 and selective catalytic reduction (SCR) retrofits, Atmos. Environ., 43, 1917-1925,
767 https://doi.org/10.1016/j.atmosenv.2008.12.040, 2009.
768 Cass, G. R.: Organic molecular tracers for particulate air pollution sources, Trac-
769 Trends in Analytical Chemistry, 17, 356-366, 10.1016/s0165-9936(98)00040-5, 1998.
770 Corbin, J. C., Pieber, S. M., Czech, H., Zanatta, M., Jakobi, G., Massabò, D.,
771 Orasche, J., El Haddad, I., Mensah, A. A., Stengel, B., Drinovec, L., Mocnik, G.,
772 Zimmermann, R., Prévôt, A. S. H., and Gysel, M.: Brown and Black Carbon Emitted
773 by a Marine Engine Operated on Heavy Fuel Oil and Distillate Fuels: Optical Properties,
774 Size Distributions, and Emission Factors, J. Geophys. Res.-Atmos., 123, 6175-6195,
775 https://doi.org/10.1029/2017JD027818, 2018.
776 Davis, D. D., Grodzinsky, G., Kasibhatla, P., Crawford, J., Chen, G., Liu, S., Bandy,
777 A., Thornton, D., Guan, H., and Sandholm, S.: Impact of ship emissions on marine
778 boundary layer NO_x and SO_2 distributions over the Pacific basin, Geophys. Res. Lett.,
779 28, 235-238, Doi 10.1029/2000gl012013, 2001.
780 Dinamarca, M. A., Rojas, A., Baeza, P., Espinoza, G., Ibacache-Quiroga, C., and
781 Ojeda, J.: Optimizing the biodesulfurization of gas oil by adding surfactants to
782 immobilized cell systems, Fuel., 116, 237-241, 10.1016/j.fuel.2013.07.108, 2014.
783 Drozd, G. T., Zhao, Y., Saliba, G., Frodin, B., Maddox, C., Oliver Chang, M. C.,
784 Maldonado, H., Sardar, S., Weber, R. J., Robinson, A. L., and Goldstein, A. H.: Detailed
785 Speciation of Intermediate Volatility and Semivolatile Organic Compound Emissions
786 from Gasoline Vehicles: Effects of Cold-Starts and Implications for Secondary Organic
787 Aerosol Formation, Environ. Sci. Technol., 53, 1706-1714, 10.1021/acs.est.8b05600,
788 2019.
789 Drozd, G. T., Weber, R. J., and Goldstein, A. H.: Highly Resolved Composition
790 during Diesel Evaporation with Modeled Ozone and Secondary Aerosol Formation:
791 Insights into Pollutant Formation from Evaporative Intermediate Volatility Organic
792 Compound Sources, Environ. Sci. Technol., 55, 5742-5751, 10.1021/acs.est.0c08832,
793 2021.
794 Duan, F., He, K., and Liu, X.: Characteristics and source identification of fine
795 particulate n-alkanes in Beijing, China, JEnvS, 22, 998-1005, 10.1016/s1001-
796 0742(09)60210-2, 2010.
797 Faber, J., Hanayama, S., Zhang, S., Pereda, P., Comer, B., Hauerhof, E., van der
798 Loeff, W. S., Smith, T., Zhang, Y., and Kosaka, H.: Fourth IMO GHG Study, London,
799 UK, 2020.
800 Fang, Z., Li, C., He, Q., Czech, H., Groger, T., Zeng, J., Fang, H., Xiao, S., Pardo,
801 M., Hartner, E., Meidan, D., Wang, X., Zimmermann, R., Laskin, A., and Rudich, Y.:
802 Secondary organic aerosols produced from photochemical oxidation of secondarily
803 evaporated biomass burning organic gases: Chemical composition, toxicity, optical
804 properties, and climate effect, Environ. Int., 157, 106801,
805 10.1016/j.envint.2021.106801, 2021.
806 Fujitani, Y., Sato, K., Tanabe, K., Takahashi, K., Hoshi, J., Wang, X., Chow, J. C.,
807 and Watson, J. G.: Volatility Distribution of Organic Compounds in Sewage
808 Incineration Emissions, Environ. Sci. Technol., 54, 14235-14245,
809 10.1021/acs.est.0c04534, 2020.
810 Hamada, H., and Haneda, M.: A review of selective catalytic reduction of nitrogen
811 oxides with hydrogen and carbon monoxide, Applied Catalysis A: General, 421-422, 1-
812 13, https://doi.org/10.1016/j.apcata.2012.02.005, 2012.
813 He, X., Zheng, X., You, Y., Zhang, S. J., Zhao, B., Wang, X., Huang, G. H., Chen,
814 T., Cao, Y. H., He, L. Q., Chang, X., Wang, S. X., and Wu, Y.: Comprehensive chemical
815 characterization of gaseous I/SVOC emissions from heavy-duty diesel vehicles using

two-dimensional gas chromatography time-of-flight mass spectrometry, Environ. Pollut., 305, ARTN 119284
10.1016/j.envpol.2022.119284, 2022a.
He, X., Zheng, X., Zhang, S., Wang, X., Chen, T., Zhang, X., Huang, G., Cao, Y., He, L., Cao, X., Cheng, Y., Wang, S., and Wu, Y.: Comprehensive characterization of particulate intermediate-volatility and semi-volatile organic compounds (I/SVOCs) from heavy-duty diesel vehicles using two-dimensional gas chromatography time-of-flight mass spectrometry, Atmos. Chem. Phys., 22, 13935-13947, 10.5194/acp-22-13935-2022, 2022b.
He, K., Shen, Z., Zhang, L., Wang, X., Zhang, B., Sun, J., Xu, H., Hang Ho, S. S., and Cao, J.-j.: Emission of Intermediate Volatile Organic Compounds from Animal Dung and Coal Combustion and Its Contribution to Secondary Organic Aerosol Formation in Qinghai-Tibet Plateau, China, Environ. Sci. Technol., 58, 11118-11127, 10.1021/acs.est.4c02618, 2024.
He, K., Fu, T., Zhang, B., Xu, H. M., Sun, J., Zou, H. J., Zhang, Z., Ho, S. S. H., Cao, J. J., and Shen, Z. X.: Examination of long-time aging process on volatile organic compounds emitted from solid fuel combustion in a rural area of China, Chemosphere, 333, ARTN
138957,10.1016/j.chemosphere.2023.138957, 2023.
Hu, C., Yue, F., Zhan, H., Leung, K. M. Y., Zhang, R., Gu, W., Liu, H., Chen, A., Cao, Y., Wang, X., and Xie, Z.: Homologous series of n-alkanes and fatty acids in the summer atmosphere from the Bering Sea to the western North Pacific, Atmos. Res., 285, 106633, https://doi.org/10.1016/j.atmosres.2023.106633, 2023.
Huang, C., Hu, Q., Wang, H., Qiao, L., Jing, S. a., Wang, H., Zhou, M., Zhu, S., Ma, Y., Lou, S., Li, L., Tao, S., Li, Y., and Lou, D.: Emission factors of particulate and gaseous compounds from a large cargo vessel operated under real-world conditions, Environ. Pollut., 242, 667-674, https://doi.org/10.1016/j.envpol.2018.07.036, 2018a.
Huang, C., Hu, Q. Y., Li, Y. J., Tian, J. J., Ma, Y. G., Zhao, Y. L., Feng, J. L., An, J. Y., Qiao, L. P., Wang, H. L., Jing, S. A., Huang, D. D., Lou, S. R., Zhou, M., Zhu, S. H., Tao, S. K., and Li, L.: Intermediate Volatility Organic Compound Emissions from a Large Cargo Vessel Operated under Real-World Conditions, Environ. Sci. Technol., 52, 12934-12942, 10.1021/acs.est.8b04418, 2018b.
Hui, L., Liu, X., Tan, Q., Feng, M., An, J., Qu, Y., Zhang, Y., and Cheng, N.: VOC characteristics, sources and contributions to SOA formation during haze events in Wuhan, Central China, Sci. Total. Environ., 650, 2624-2639, 10.1016/j.scitotenv.2018.10.029, 2019.
Ju, H.-j., and Jeon, S.-k.: Analysis of Characteristic Changes of Blended Very Low Sulfur Fuel Oil on Ultrasonic Frequency for Marine Fuel, J. Mar. Sci. Eng., 10, 1254, 2022.
International Maritime Organization, 2016. International Convention for the Prevention of Pollution from Ships, in: International Maritime Organization (Ed.)
Kawamura, K., Matsumoto, K., Uchida, M., and Shibata, Y.: Contributions of modern and dead organic carbon to individual fatty acid homologues in spring aerosols collected from northern Japan, J. Geophys. Res-Atmos., 115, Artn D22310
10.1029/2010jd014515, 2010.
Kawamura, K., Hoque, M. M. M., Bates, T. S., and Quinn, P. K.: Molecular distributions and isotopic compositions of organic aerosols over the western North Atlantic: Dicarboxylic acids, related compounds, sugars, and secondary organic aerosol tracers, Org. Geochem., 113, 229-238, https://doi.org/10.1016/j.orggeochem.2017.08.007, 2017.

Kleeman, M. J., Riddle, S. G., Robert, M. A., and Jakober, C. A.: Lubricating oil and fuel contributions to particulate matter emissions from light-duty gasoline and heavy-duty diesel vehicles, Environ. Sci. Technol., 42, 235-242, 10.1021/es071054c, 2008.

Knote, C., Hodzic, A., and Jimenez, J. L.: The effect of dry and wet deposition of condensable vapors on secondary organic aerosols concentrations over the continental US, Atmos. Chem. Phys., 15, 1-18, 10.5194/acp-15-1-2015, 2015.

Kramel, D., Muri, H., Kim, Y., Lonka, R., Nielsen, J. B., Ringvold, A. L., Bouman, E. A., Steen, S., and Strømman, A. H.: Global Shipping Emissions from a Well-to-Wake Perspective: The MariTEAM Model, Environ. Sci. Technol., 55, 15040-15050, 10.1021/acs.est.1c03937, 2021.

Lehtoranta, K., Aakko-Saksa, P., Murtonen, T., Vesala, H., Ntziachristos, L., Ronkko, T., Karjalainen, P., Kuittinen, N., and Timonen, H.: Particulate Mass and Nonvolatile Particle Number Emissions from Marine Engines Using Low-Sulfur Fuels, Natural Gas, or Scrubbers, Environ. Sci. Technol., 53, 3315-3322, 10.1021/acs.est.8b05555, 2019.

Li, J., Zhang, Q., Wang, G., Li, J., Wu, C., Liu, L., Wang, J., Jiang, W., Li, L., Ho, K. F., and Cao, J.: Optical properties and molecular compositions of water-soluble and water-insoluble brown carbon (BrC) aerosols in northwest China, Atmos. Chem. Phys., 20, 4889-4904, 10.5194/acp-20-4889-2020, 2020.

Li, J. J., Wang, G. H., Ren, Y. Q., Wang, J. Y., Wu, C., Han, Y. N., Zhang, L., Cheng, C. L., and Meng, J. J.: Identification of chemical compositions and sources of atmospheric aerosols in Xi'an, inland China during two types of haze events, Sci. Total. Environ., 566, 230-237, 10.1016/j.scitotenv.2016.05.057, 2016.

Liang, Z., Yu, Z., Zhang, C., and Chen, L.: IVOC/SVOC and size distribution characteristics of particulate matter emissions from a modern aero-engine combustor in different operational modes, Fuel., 314, 10.1016/j.fuel.2021.122781, 2022.

Liu, H., Meng, Z.-H., Lv, Z.-F., Wang, X.-T., Deng, F.-Y., Liu, Y., Zhang, Y.-N., Shi, M.-S., Zhang, Q., and He, K.-B.: Emissions and health impacts from global shipping embodied in US-China bilateral trade, Nat. Sustain., 2, 1027-1033, 10.1038/s41893-019-0414-z, 2019.

Liu, Z. Y., Chen, Y. J., Zhang, Y., Zhang, F., Feng, Y. L., Zheng, M., Li, Q., and Chen, J. M.: Emission Characteristics and Formation Pathways of Intermediate Volatile Organic Compounds from Ocean-Going Vessels: Comparison of Engine Conditions and Fuel Types, Environ. Sci. Technol., 56, 12917-12925, 10.1021/acs.est.2c03589, 2022.

Lou, H., Hao, Y., Zhang, W., Su, P., Zhang, F., Chen, Y., Feng, D., and Li, Y.: Emission of intermediate volatility organic compounds from a ship main engine burning heavy fuel oil, J. Environ. Sci., 84, 197-204, 10.1016/j.jes.2019.04.029, 2019.

Mochida, M., Kitamori, Y., Kawamura, K., Nojiri, Y., and Suzuki, K.: Fatty acids in the marine atmosphere: Factors governing their concentrations and evaluation of organic films on sea-salt particles, J. Geophys. Res-Atmos., 107, Artn 4325
10.1029/2001jd001278, 2002.

Mochida, M., Kawamura, K., Umemoto, N., Kobayashi, M., Matsunaga, S., Lim, H. J., Turpin, B. J., Bates, T. S., and Simoneit, B. R. T.: Spatial distributions of oxygenated organic compounds (dicarboxylic acids, fatty acids, and levoglucosan) in marine aerosols over the western Pacific and off the coast of East Asia: Continental outflow of organic aerosols during the ACE-Asia campaign, J. Geophys. Res-Atmos., 108, Artn 8638
10.1029/2002jd003249, 2003.

Murphy, B. N., Woody, M. C., Jimenez, J. L., Carlton, A. M. G., Hayes, P. L., Liu, S., Ng, N. L., Russell, L. M., Setyan, A., Xu, L., Young, J., Zaveri, R. A., Zhang, Q., and Pye, H. O. T.: Semivolatile POA and parameterized total combustion SOA in CMAQv5.2: impacts on source strength and partitioning, Atmos. Chem. Phys., 17, 11107-11133, 10.5194/acp-17-11107-2017, 2017.

Nadanakumar, V., Jenoris Muthiya, S., Prudhvi, T., Induja, S., Sathyamurthy, R., and Dharmaraj, V.: Experimental investigation to control HC, CO & NO_x emissions from diesel engines using diesel oxidation catalyst, Materials Today: Proceedings, 43, 434-440, https://doi.org/10.1016/j.matpr.2020.11.964, 2021.

Organization, I. M.: International Convention for the Prevention of Pollution from Ships, 2016.

Perrone, M. G., Carbone, C., Faedo, D., Ferrero, L., Maggioni, A., Sangiorgi, G., and Bolzacchini, E.: Exhaust emissions of polycyclic aromatic hydrocarbons, n-alkanes and phenols from vehicles coming within different European classes, Atmos. Environ., 82, 391-400, https://doi.org/10.1016/j.atmosenv.2013.10.040, 2014.

Reşitoğlu, İ. A., Altinişik, K., and Keskin, A.: The pollutant emissions from diesel-engine vehicles and exhaust aftertreatment systems, Clean Technol. Environ. Policy, 17, 15-27, 10.1007/s10098-014-0793-9, 2015.

Robinson, A. L., Donahue, N. M., Shrivastava, M. K., Weitkamp, E. A., Sage, A. M., Grieshop, A. P., Lane, T. E., Pierce, J. R., and Pandis, S. N.: Rethinking organic aerosols: Semivolatile emissions and photochemical aging, Science, 315, 1259-1262, 10.1126/science.1133061, 2007.

Schüppel, M., and Gräbner, M.: Pyrolysis of heavy fuel oil (HFO) – A review on physicochemical properties and pyrolytic decomposition characteristics for application in novel, industrial-scale HFO pyrolysis technology, J. Anal. Appl. Pyrolysis, 179, 106432, 10.1016/j.jaap.2024.106432, 2024.

Shen, X. B., Che, H. Q., Yao, Z. L., Wu, B. B., Lv, T. T., Yu, W. H., Cao, X. Y., Hao, X. W., Li, X., Zhang, H. Y., and Yao, X. L.: Real-World Emission Characteristics of Full-Volatility Organics Originating from Nonroad Agricultural Machinery during Agricultural Activities, Environ. Sci. Technol., 57, 10308-10318, 10.1021/acs.est.3c02619, 2023.

Shrivastava, P., and Nath Verma, T.: An experimental investigation into engine characteristics fueled with Lal ambari biodiesel and its blends, Therm. Sci. Eng. Prog., 17, 100356, https://doi.org/10.1016/j.tsep.2019.100356, 2020.

Sofiev, M., Winebrake, J. J., Johansson, L., Carr, E. W., Prank, M., Soares, J., Vira, J., Kouznetsov, R., Jalkanen, J. P., and Corbett, J. J.: Cleaner fuels for ships provide public health benefits with climate tradeoffs, Nat. Commun., 9, 10.1038/s41467-017-02774-9, 2018.

Srivastava, D., Vu, T. V., Tong, S. R., Shi, Z. B., and Harrison, R. M.: Formation of secondary organic aerosols from anthropogenic precursors in laboratory studies, npj Clim. Atmos. Sci., 5, 10.1038/s41612-022-00238-6, 2022.

Su, P., Hao, Y., Qian, Z., Zhang, W., Chen, J., Zhang, F., Yin, F., Feng, D., Chen, Y., and Li, Y.: Emissions of intermediate volatility organic compound from waste cooking oil biodiesel and marine gas oil on a ship auxiliary engine, J. Environ. Sci., 91, 262-270, 10.1016/j.jes.2020.01.008, 2020.

Wang, H., Hu, Q., Huang, C., Lu, K., He, H., and Peng, Z.: Quantification of Gaseous and Particulate Emission Factors from a Cargo Ship on the Huangpu River, in: J. Mar. Sci. Eng., 8, 2023.

Watson, J. G., Chow, J. C., Lowenthal, D. H., Pritchett, L. C., Frazier, C. A., Neuroth, G. R., and Robbins, R.: Differences in the carbon composition of source

profiles for diesel- and gasoline-powered vehicles, Atmos. Environ., 28, 2493-2505, https://doi.org/10.1016/1352-2310(94)90400-6, 1994.

Wu, L., Wang, X., Lu, S., Shao, M., and Ling, Z.: Emission inventory of semi-volatile and intermediate-volatility organic compounds and their effects on secondary organic aerosol over the Pearl River Delta region, Atmos. Chem. Phys., 19, 8141-8161, 10.5194/acp-19-8141-2019, 2019.

Wu, Z., Zhang, Y., He, J., Chen, H., Huang, X., Wang, Y., Yu, X., Yang, W., Zhang, R., Zhu, M., Li, S., Fang, H., Zhang, Z., and Wang, X.: Dramatic increase in reactive volatile organic compound (VOC) emissions from ships at berth after implementing the fuel switch policy in the Pearl River Delta Emission Control Area, Atmos. Chem. Phys., 20, 1887-1900, 10.5194/acp-20-1887-2020, 2020.

Xie, M., Wang, G., Hu, S., Han, Q., Xu, Y., and Gao, Z.: Aliphatic alkanes and polycyclic aromatic hydrocarbons in atmospheric PM_{10} aerosols from Baoji, China: Implications for coal burning, Atmos. Res., 93, 840-848, https://doi.org/10.1016/j.atmosres.2009.04.004, 2009.

Yashnik, S. A., and Ismagilov, Z. R.: Diesel Oxidation Catalyst Pt–Pd/MnO_x–Al_2O_3 for Soot Emission Control: Effect of NO and Water Vapor on Soot Oxidation, Topics in Catalysis, 66, 860-874, 10.1007/s11244-022-01779-z, 2023.

Yu, G. Y., Zhang, Y., Yang, F., He, B. S., Zhang, C. G., Zou, Z., Yang, X., Li, N., and Chen, J.: Dynamic Ni/V Ratio in the Ship-Emitted Particles Driven by Multiphase Fuel Oil Regulations in Coastal China, Environ. Sci. Technol., 55, 15031-15039, 10.1021/acs.est.1c02612, 2021.

Zhang, F., Chen, Y. J., Tian, C. G., Wang, X. P., Huang, G. P., Fang, Y., and Zong, Z.: Identification and quantification of shipping emissions in Bohai Rim, China, Sci. Total. Environ., 497, 570-577, 10.1016/j.scitotenv.2014.08.016, 2014.

Zhang, F., Chen, Y. J., Tian, C. G., Lou, D. M., Li, J., Zhang, G., and Matthias, V.: Emission factors for gaseous and particulate pollutants from offshore diesel engine vessels in China, Atmos. Chem. Phys., 16, 6319-6334, 10.5194/acp-16-6319-2016, 2016.

Zhang, F., Chen, Y., Chen, Q., Feng, Y., shang, Y., Yang, X., Gao, H., Tian, C., Li, J., Zhang, G., Matthias, V., and Xie, Z.: Real-World Emission Factors of Gaseous and Particulate Pollutants from Marine Fishing Boats and Their Total Emissions in China, Environ. Sci. Technol., 52, 4910-4919, 10.1021/acs.est.7b04002, 2018a.

Zhang, F., Chen, Y. J., Su, P. H., Cui, M., Han, Y., Matthias, V., and Wang, G. H.: Variations and characteristics of carbonaceous substances emitted from a heavy fuel oil ship engine under different operating loads, Environ. Pollut., 284, ARTN 117388 10.1016/j.envpol.2021.117388, 2021.

Zhang, F., Xiao, B., Liu, Z., Zhang, Y., Tian, C., Li, R., Wu, C., Lei, Y., Zhang, S., Wan, X., Chen, Y., Han, Y., Cui, M., Huang, C., Wang, H., Chen, Y., and Wang, G.: Real-world emission characteristics of VOCs from typical cargo ships and their potential contributions to secondary organic aerosol and O_3 under low-sulfur fuel policies, Atmos. Chem. Phys., 24, 8999-9017, 10.5194/acp-24-8999-2024, 2024.

Zhang, Y., Yang, W., Simpson, I., Huang, X., Yu, J., Huang, Z., Wang, Z., Zhang, Z., Liu, D., Huang, Z., Wang, Y., Pei, C., Shao, M., Blake, D. R., Zheng, J., Huang, Z., and Wang, X.: Decadal changes in emissions of volatile organic compounds (VOCs) from on-road vehicles with intensified automobile pollution control: Case study in a busy urban tunnel in south China, Environ. Pollut., 233, 806-819, 10.1016/j.envpol.2017.10.133, 2018b.

Zhao, W., Zhang, Y., Huang, G., He, Z., Qian, Y., and Lu, X.: Experimental study of butanol/biodiesel dual-fuel combustion in intelligent charge compression ignition

(ICCI) mode: A systematic analysis at low load, Fuel., 287, 119523, https://doi.org/10.1016/j.fuel.2020.119523, 2021.

Zhao, J. C., Qi, L. J., Lv, Z. F., Wang, X. T., Deng, F. Y., Zhang, Z. N., Luo, Z. Y., Bie, P. J., He, K. B., and Liu, H.: An updated comprehensive IVOC emission inventory for mobile sources in China, Sci. Total. Environ., 851, ARTN 158312, 10.1016/j.scitotenv.2022.158312, 2022.

Zhao, Y., Hennigan, C. J., May, A. A., Tkacik, D. S., de Gouw, J. A., Gilman, J. B., Kuster, W. C., Borbon, A., and Robinson, A. L.: Intermediate-Volatility Organic Compounds: A Large Source of Secondary Organic Aerosol, Environ. Sci. Technol., 48, 13743-13750, 10.1021/es5035188, 2014.

Zhao, Y., Nguyen, N. T., Presto, A. A., Hennigan, C. J., May, A. A., and Robinson, A. L.: Intermediate Volatility Organic Compound Emissions from On-Road Diesel Vehicles: Chemical Composition, Emission Factors, and Estimated Secondary Organic Aerosol Production, Environ. Sci. Technol., 49, 11516-11526, 10.1021/acs.est.5b02841, 2015.

Zhao, Y., Nguyen, N. T., Presto, A. A., Hennigan, C. J., May, A. A., and Robinson, A. L.: Intermediate Volatility Organic Compound Emissions from On-Road Gasoline Vehicles and Small Off-Road Gasoline Engines, Environ. Sci. Technol., 50, 4554-4563, 10.1021/acs.est.5b06247, 2016.

Zhou, S., Zhou, J., and Zhu, Y.: Chemical composition and size distribution of particulate matters from marine diesel engines with different fuel oils, Fuel., 235, 972-983, 10.1016/j.fuel.2018.08.080, 2019.